Global Health Care
WISDOM ACADEMIC https://doi.org/10.63808/ghc.v2i1.540 Volume 2 , Issue 1

Research Article

Overcoming Anti-PD-1 Resistance: Targeted STING Activation Reprograms Tumor-Associated Macrophages

Gang Liu[1,*], Jia Wang[2], Alena Mikalaeuna Vasiukevich[1]
[1]International Sakharov Environmental Institute, Belarusian State University, Minsk 220114, Belarus
[2]Taishan Polytechnic, Tai'an 271000, China
[*]**Correspondence:** Gang Liu, lg6666699@163.com

© The Author(s) 2026.
This article is published by Wisdom Academic Press Ltd. under a Creative Commons Attribution 4.0 International License. The license permits use, sharing, adaptation, distribution, and reproduction in any medium or format, provided that appropriate credit is given to the original author(s) and the source, a link to the license is supplied, and any modifications are indicated. Unless otherwise stated, all images and third-party materials included in this article are also covered by the same license. For any material not covered by this license, if the intended use is neither permitted by applicable law nor allowed under the license terms, direct permission must be obtained from the copyright holder. To view a copy of this license, please visit http://creativecommons.org/licenses/by/4.0/.

Abstract

Anti-PD-1 immunotherapy has limited response rates in various solid tumors, and the immunosuppressive microenvironment mediated by tumor-associated macrophages (TAMs) is a key factor leading to resistance. This study aims to explore whether targeting and activating the STING pathway can reprogram TAMs to reverse resistance to anti-PD-1 therapy. An anti-PD-1 resistant mouse transplant tumor model was established, and intratumoral injection or nanoparticle-targeted delivery of a STING agonist was used. Flow cytometry, multiplex immunohistochemistry, transcriptome sequencing, and other methods were employed to analyze TAM polarization phenotypes, cytokine expression, and tumor-infiltrating lymphocyte function, as well as to systematically evaluate the antitumor effect of STING agonist combined with anti-PD-1 therapy. STING activation significantly promoted the conversion of TAMs from an immunosuppressive M2 phenotype to a pro-inflammatory M1 phenotype, upregulated the expression of MHC-II, CD86, and type I interferon-related genes, and enhanced antigen-presenting capability; at the same time, it remodeled the tumor microenvironment, increased CD8 T cell infiltration and granzyme B and IFN-γ secretion, and reduced the proportion of regulatory T cells. In the resistant model, STING agonist combined with anti-PD-1 therapy significantly inhibited tumor growth and prolonged mouse survival compared with monotherapy, with some mice achieving complete tumor regression. Targeting the STING pathway can reprogram TAMs to remodel the tumor immune microenvironment and effectively overcome resistance to anti-PD-1 therapy, providing a new strategy for clinical combination immunotherapy.

Keywords

Anti-PD-1 resistance, STING, Tumor-associated macrophages, Immune reprogramming, Tumor microenvironment

1. Introduction

The use of immune checkpoint inhibitors (ICIs) has profoundly changed the landscape of cancer treatment. Monoclonal antibodies targeting programmed cell death protein 1 (PD-1) and its ligand (PD-L1) are a prime example and have shown lasting clinical benefits in various solid tumors, including melanoma, non-small cell lung cancer, and renal cell carcinoma. However, even among patients who initially respond, a considerable number eventually develop primary or acquired resistance, and the overall objective response rate hovers around only 20%–40% for most cancers. This clinical bottleneck urgently calls for a deeper understanding of the molecular mechanisms behind anti-PD-1 resistance and exploring combination therapies that can effectively overcome this resistance.

Tumor-associated macrophages (TAMs) are one of the most abundant immune cell types in the tumor microenvironment (TME) and play a key role in tumor progression and immune evasion. Under the influence of tumor-derived cytokines like IL-4, IL-10, and M-CSF, TAMs often get polarized into an immunosuppressive M2-like state, expressing high levels of inhibitory molecules such as IL-10, TGF-β, and arginase-1 (Arg-1), while showing low levels of MHC-II and co-stimulatory molecules. This suppresses CD8 T cell activation and function and recruits regulatory T cells (Tregs) and myeloid-derived suppressor cells (MDSCs). Clinical evidence shows that high TAM infiltration is significantly linked to poor response to anti-PD-1 therapy and worse prognosis. So, reprogramming TAMs from the immunosuppressive M2-like state to a pro-inflammatory M1-like state has become an important research direction for overcoming anti-PD-1 resistance.

The stimulatory of interferon genes (STING) is a key adaptor protein in the cytoplasmic DNA sensing pathway cGAS-STING. It plays a role in innate immunity by recognizing cytoplasmic double-stranded DNA and inducing type I interferons (IFN-I) and various pro-inflammatory cytokines. In recent years, STING agonists have gained widespread attention as a new kind of anti-tumor immunotherapy. They can not only directly activate dendritic cells (DCs) to boost T cell priming but also promote immunogenic death of tumor cells. However, the direct role of STING signaling in TAMs and its effect on reshaping PD-1 resistant tumor microenvironments still lack systematic study. There is preliminary evidence that STING activation can drive macrophages toward a pro-inflammatory phenotype, upregulate MHC-II and co-stimulatory molecules, and enhance antigen presentation. But whether this effect is enough to reverse an established PD-1 resistant state in vivo, its downstream molecular mechanisms, and how it works together with T cells remain unclear.

Based on the research background above, this study proposes a scientific hypothesis: targeting STING activation could reprogram TAMs and reshape the immunosuppressive tumor microenvironment, thereby restoring T cell anti-tumor activity and overcoming resistance to anti-PD-1

therapy. To test this hypothesis, we built a mouse transplant tumor model resistant to anti-PD-1, systematically evaluated the effects of STING agonists on TAM phenotype and function, and further explored the anti-tumor effects and mechanisms of combining STING agonists with anti-PD-1 treatment. This study aims to provide theoretical and experimental support for combination immunotherapy strategies based on the STING-TAMs axis.

2. Literature Review

Anti-PD-1/PD-L1 immune checkpoint blockade therapy has reshaped the treatment landscape for various malignant tumors, but primary and acquired resistance remain the main barriers limiting its clinical benefits (Pitt et al., 2016; Sharma et al., 2017). The mechanisms of drug resistance are complex and varied, involving abnormal signals inside tumor cells, defects in antigen presentation, T cell exhaustion, and the remodeling of the immunosuppressive tumor microenvironment (TME), among other things (Chen & Mellman, 2013; Kalbasi & Ribas, 2020). Among them, tumor-associated macrophages (TAMs), as the most abundant innate immune cell population infiltrating the TME, play a key role in mediating immune evasion and therapy resistance (Mantovani et al., 2017; Ruffell & Coussens, 2015).

2.1. Tumor-associated macrophages and anti-PD-1 resistance

TAMs are really flexible, and when influenced by tumor-derived cytokines like IL-4, IL-10, and M-CSF, they usually shift into an M2-like immunosuppressive type. They crank up the levels of inhibitory molecules like IL-10, TGF-β, and arginase-1 (Arg-1), while keeping MHC-II and co-stimulatory molecules CD80/CD86 low (Liu & Cao, 2015; Murray et al., 2014). This phenotype not only directly suppresses the proliferation and effector functions of CD8 T cells, but also recruits regulatory T cells (Tregs) and myeloid-derived suppressor cells (MDSCs) by secreting chemokines, further intensifying immune suppression (DeNardo & Ruffell, 2019). Clinical pathological analysis shows that high infiltration of TAMs is significantly linked to a low response rate to anti-PD-1 treatment and poor prognosis, and the immunosuppressive factors from TAMs can weaken the ability of T cells to reactivate after PD-1 blockade (Cassetta & Pollard, 2018; Peranzoni et al., 2018). So, reprogramming TAMs from an M2-like state to a pro-inflammatory M1-like state is considered one of the feasible strategies to reverse anti-PD-1 resistance (Kowal et al., 2019).

2.2. The dual role of the STING signaling pathway in tumor immunity

The cGAS-STING pathway is a key mechanism for sensing DNA in the cytoplasm. It can detect tumor-derived cytoplasmic DNA and trigger the production of type I interferons (IFN-I) and various pro-inflammatory cytokines, thus linking innate immunity with adaptive immunity (Barber, 2015; Li

& Chen, 2018). In tumor models, STING agonists can boost tumor antigen cross-presentation by activating dendritic cells (DCs), which helps kickstart CD8 T cells and promotes tumor infiltration, leading to a strong anti-tumor effect (Corrales et al., 2015; Woo et al., 2014). In addition, STING activation can also trigger immunogenic cell death in tumor cells, releasing damage-associated molecular patterns (DAMPs) and further boosting the immune response (Deng et al., 2014). However, the role of STING signaling in tumor immunity depends on the context: chronic STING activation might promote tumor progression by inducing immune-suppressive molecules or promoting tolerogenic DCs (Gulen et al., 2017). This complexity suggests that STING-targeted therapy needs careful control of activation strength and timing.

2.3. Interaction between STING and macrophages

Macrophages highly express STING, and STING activators can directly drive macrophages toward a pro-inflammatory phenotype, upregulating genes like MHC-II, CD86, and IFN-β, CXCL10, and so on (Cheng et al., 2018; Ohkuri et al., 2014). In lab experiments, activating STING can counteract IL-4-induced M2 polarization, reduce Arg-1 and CD206 expression, and restore the antigen-presenting ability of macrophages (Downey et al., 2014). Inside the body, STING agonists can reshape the transcriptomic profile of TAMs, reducing M2-related gene signatures, boosting M1-related pro-inflammatory gene expression, and enhancing the effector function of CD8 T cells (Sivick et al., 2018). However, most studies use tumor models with strong immunogenicity or don't fully take into account the background of anti-PD-1 resistance, so there's still no direct evidence that STING activation can effectively reprogram TAMs and restore T cell responses in an established resistant microenvironment.

2.4. Current research on combining STING agonists with anti-PD-1 therapy

Multiple preclinical studies have shown that combining STING agonists with anti-PD-1 antibodies can produce a synergistic anti-tumor effect. For example, injecting STING agonists directly into tumors along with systemic anti-PD-1 treatment can lead to the shrinkage of both local and distant tumors and establish long-term immune memory (Fu et al., 2015). In TNBC models that aren't sensitive to PD-L1, delivering STING agonists with nanoparticles can boost the effect of anti-PD-L1 therapy, and some animals even had complete tumor regression (Cheng et al., 2018). These studies suggest that activating STING might help overcome resistance to immune checkpoint blockade by reshaping the immune microenvironment. However, most current combination therapy studies focus on models that are initially sensitive or partially sensitive to immunotherapy, and there's still a lack of systematic research on using STING agonists specifically in tumor models that have already developed resistance to anti-PD-1.

2.5. Limitations of existing research and contributions of this study

In summary, although the important role of the STING pathway in anti-tumor immunity is widely recognized, several key questions remain unresolved: Is the direct reprogramming effect of STING activation on TAMs enough to reverse an established immunosuppressive environment in anti-PD-1 resistant models? The anti-tumor effects and cellular mechanisms of combining STING agonists with anti-PD-1 antibodies in resistant settings are still unclear; and the causal relationship between TAM phenotype changes and T cell function recovery lacks in vivo functional validation.

To address the above gaps, this study established a PD-1 resistant mouse transplant tumor model and systematically evaluated how STING agonists affect TAM polarization, antigen-presenting function, and cytokine networks. We also used combination therapy experiments to analyze the synergistic anti-tumor effects of STING agonists and anti-PD-1, as well as the immune cell subsets involved. The contribution of this study is that, for the first time in a PD-1 resistant model, it shows that STING-mediated TAM reprogramming is enough to restore T cell anti-tumor activity, providing direct experimental evidence for combination immunotherapy strategies based on the STING-TAM axis.

3. Materials and Methods

3.1. Experimental animals and ethics statement

We used female SPF-grade C57BL/6J mice, aged 6-8 weeks and weighing 18-22 g, bought from Beijing Vital River Laboratory Animal Technology Co., Ltd. The mice were kept in a cozy SPF-quality environment with a stable temperature (22 ± 2°C), humidity (55% ± 5%), and a 12-hour light-dark cycle, having free access to food and water. All animal experiments were approved by our institution's animal ethics committee and followed the ARRIVE guidelines and 'Guidelines for the Management and Use of Laboratory Animals' strictly. This study has been approved by the Ethics Committee of Belarusian State University (Approval No: BSU-DHF-2026-0311), and all participants signed written informed consent forms.

3.2. Cell lines and culture conditions

The mouse colon cancer cell line MC38 was purchased from the American Type Culture Collection (ATCC). The cells were cultured in high-glucose DMEM (HyClone) containing 10% fetal bovine serum (FBS, Gibco), 100 U/mL penicillin, and 100 μg/mL streptomycin, and kept in a 37°C incubator with 5% CO_2. The cells were passaged every 2–3 days, and cells in the logarithmic growth phase were used for subsequent experiments. All cells were confirmed by short tandem repeat (STR) profiling and regularly tested negative for mycoplasma contamination.

3.3. Establishing PD-1 resistant cell lines

The PD-1-resistant MC38 cell line (MC38-R) was obtained through continuous in vivo selection. The process was as follows: 1×10^6 MC38 cells were suspended in 100 μL of PBS and injected subcutaneously into the right flank of C57BL/6J mice. When tumor volumes reached 80-100 mm^3, anti-mouse PD-1 antibody (clone RMP1-14, Bio X Cell, 200 μg per mouse, every 3 days for 4 doses) was administered intraperitoneally. Mice whose tumors continued to grow (tumor volume >500 mm^3) after treatment were considered resistant. The mice were euthanized, and tumor tissues were aseptically isolated, minced, and digested in RPMI-1640 containing 1 mg/mL collagenase IV (Sigma) and 0.1 mg/mL DNase I (Sigma) at 37°C for 30 minutes. The digested tissue was filtered through a 70 μm mesh to obtain a single-cell suspension. Tumor cells were then cultured in DMEM with 10% FBS, and fibroblasts and immune cells were removed by differential adhesion to obtain purified tumor cells. These tumor cells were expanded and re-injected into a new batch of C57BL/6J mice (1×10^6 per mouse), repeating the anti-PD-1 treatment and resistance selection process. After three rounds of in vivo selection, a stable PD-1-resistant cell line, MC38-R, was established. The resistant phenotype was confirmed by comparing tumor growth curves and survival between MC38 and MC38-R under anti-PD-1 treatment.

3.4. Establishment of animal models and group administration

Female C57BL/6J mice were randomly divided into 4 groups (8-10 mice per group): the control group (PBS and isotype control antibody), the STING agonist monotherapy group, the anti-PD-1 monotherapy group, and the STING agonist plus anti-PD-1 combination group. MC38-R cells (1×10^6 per mouse) were subcutaneously injected into the right flank of the mice. Treatment started when the tumor volume reached 50-100 mm^3. The dosing regimen was as follows: STING agonist: DMXAA (5,6-dimethylxanthenone-4-acetic acid, MedChemExpress, purity ≥98%) was dissolved in sterile PBS and injected intratumorally at 25 mg/kg every 3 days for a total of 3 doses. Anti-PD-1 antibody: anti-mouse PD-1 antibody (clone RMP1-14) was injected intraperitoneally at 200 μg per mouse every 3 days for a total of 4 doses. Control group: equal volume of sterile PBS injected intratumorally and isotype control antibody (Rat IgG2a, Bio X Cell, 200 μg per mouse) injected intraperitoneally, following the same dosing schedule.

Measure the tumor's long diameter (L) and short diameter (W) with a caliper every 2 days, and calculate the tumor volume using the formula $V = (L \times W^2)/2$. If the tumor volume exceeds 2000 mm^3 or obvious ulcers appear, or if the mouse loses more than 20% of its body weight, consider it an experimental endpoint and euthanize the mouse. Record the survival time and plot a Kaplan-Meier curve.

3.5. Nanoparticle delivery of STING agonists (supporting experiment)

To evaluate the feasibility of systemically delivering STING agonists, a nanoparticle delivery group was also set up. PLGA-PEG nanoparticles were used to encapsulate DMXAA: PLGA-PEG (poly(lactic-co-glycolic acid)-polyethylene glycol, Sigma) and DMXAA were dissolved in a 10:1 weight ratio in dichloromethane, and nanoparticles were made using an ultrasonic emulsification-solvent evaporation method, with a particle size of about 150 nm, zeta potential around −15 mV, and drug loading of about 5%. The nanoparticles were injected via the tail vein, with a DMXAA equivalent dose of 5 mg/kg, once every 3 days for a total of 3 times. This group was used to assess the effects of systemic STING agonist delivery on tumors and tumor-associated macrophages.

3.6. Flow cytometry analysis

On the 7th day after the last dose, the mice were euthanized, and the tumor tissues were removed. After weighing, they were chopped into pieces about 1 mm^3 in size. Digestive solution containing 1 mg/mL collagenase IV, 0.1 mg/mL DNase I, and 5% FBS in RPMI-1640 was added, and the mixture was digested at 37°C on a shaking incubator (200 rpm) for 45 minutes. The solution was passed through a 70 μm filter, washed with PBS, and red blood cells were lysed at room temperature for 5 minutes using BD Pharm Lyse. The cells were collected by centrifugation, resuspended in PBS containing 2% FBS, and the cell density was adjusted to 1×10^7/mL.

Take 100 μL of single-cell suspension and add Fc receptor blocker (anti-CD16/32, clone 2.4G2, BD Biosciences), incubate at 4°C for 10 minutes. Then, add a mixture of fluorescently labeled antibodies and incubate at 4°C in the dark for 30 minutes. The antibody panels are as follows. Myeloid cell panel: anti-CD45-BV510 (clone 30-F11), anti-CD11b-APC-Cy7 (clone M1/70), anti-F4/80-PE-Cy7 (clone BM8), anti-MHC-II-AF700 (clone M5/114.15.2), anti-CD86-FITC (clone GL-1), anti-CD206-APC (clone C068C2). Lymphocyte panel: anti-CD45-BV510, anti-CD3-FITC (clone 17A2), anti-CD4-BV421 (clone GK1.5), anti-CD8-PerCP-Cy5.5 (clone 53-6.7). All antibodies were purchased from BioLegend or BD Biosciences. After staining, wash twice with PBS containing 2% FBS and resuspend in 300 μL PBS for analysis.

For detecting intracellular cytokines and transcription factors, after surface staining, fix and permeabilize using the Foxp3/Transcription Factor Staining Buffer Set (eBioscience). Then add anti-FoxP3-PE (clone FJK-16s), anti-IFN-γ-BV650 (clone XMG1.2), anti-granzyme B-PE-CF594 (clone GB11), or anti-Ki67-BV711 (clone B56) for intracellular staining, and incubate at 4°C in the dark for 30 minutes. After washing, resuspend and run on the machine.

Data were collected using a BD LSRFortessa flow cytometer, with at least 50,000 $CD45^+$ cells recorded per sample. The data were analyzed using FlowJo v10.8. Macrophages were defined as $CD45^+CD11b^+F4/80^+$ cells, with M1-like TAMs being $MHC\text{-}II^+CD86^+$ and M2-like TAMs being

$CD206^+$. $CD8^+$ T cell effector function was assessed by the proportion of IFN-γ^+ or granzyme B^+ cells. Tregs were defined as $CD4^+FoxP3^+$ cells.

3.7. Multiplex immunohistochemistry (mIHC)

Tumor tissues were fixed overnight with 4% paraformaldehyde, then embedded in paraffin to prepare 4 μm continuous sections. The sections were deparaffinized with xylene, hydrated through a graded ethanol series, and subjected to high-pressure antigen retrieval for 10 minutes using citrate buffer (pH 6.0). Multiplex fluorescent staining was performed using the Opal 7-color IHC Kit (Akoya Biosciences), sequentially labeling: F4/80 (rabbit polyclonal, Cell Signaling Technology) - Opal 520, CD86 (rabbit monoclonal, clone D5T6T, CST) - Opal 570, CD206 (rabbit polyclonal, Abcam) - Opal 620, CD8 (rat monoclonal, clone 4SM15, eBioscience) - Opal 690, and DAPI (nuclear staining).

Primary antibodies were incubated overnight at 4°C, and secondary antibodies were HRP-conjugated anti-rabbit/rat IgG (Akoya). Opal fluorescent dyes were incubated at room temperature for 10 minutes. Multispectral images were captured using the Vectra Polaris multispectral imaging system (Akoya) and analyzed for spectral unmixing, cell segmentation, and quantification with inForm software. For each slide, five high-power fields (40×) were randomly selected to calculate the proportion of $CD86^+$ or $CD206^+$ cells among $F4/80^+$ macrophages and the density of $CD8^+$ T cell infiltration.

3.8. Transcriptome sequencing (RNA-seq)

TAMs Sorting: On day 7 after the last dose, make a single-cell suspension from the tumor and stain with anti-CD45, CD11b, and F4/80 antibodies. Use a BD FACSAria III flow cytometer to sort $CD45^+CD11b^+F4/80^+$ cells, and check that their purity is over 95%. Collect the sorted cells straight into 1.5 mL tubes with TRIzol (Invitrogen).

RNA Extraction and Quality Check: Extract total RNA according to the TRIzol reagent instructions. Use a NanoDrop 2000 spectrophotometer to check RNA concentration and purity (A260/A280 between 1.8-2.0), and use an Agilent 2100 Bioanalyzer to check RNA integrity (RIN value ≥7.0).

Library Construction and Sequencing: We took 100 ng of total RNA and used the NEBNext Ultra II RNA Library Prep Kit (NEB) to build strand-specific cDNA libraries. After quality control with the Agilent 2100, the libraries were sequenced on the Illumina NovaSeq 6000 platform with paired-end 150 bp reads, generating at least 30 million reads per sample.

Bioinformatics analysis: The raw data were quality-checked with FastQC and aligned to the mouse reference genome mm10 using STAR v2.7.10a. Gene count matrices were generated with featureCounts, and differential expression analysis was performed with DESeq2 ($|\log_2FC| \geq 1$, padj < 0.05 considered significant). Gene set enrichment analysis (GSEA) was done using the clusterProfiler

R package, referencing Hallmark gene sets in the MSigDB database and gene signatures related to macrophage polarization. Heatmaps were plotted with pheatmap, and principal component analysis (PCA) was done using built-in R functions.

3.9. Statistical analysis

All data are shown as mean ± SEM and statistical analysis was done using GraphPad Prism 8.0. Comparisons between two groups were made using Student's t-test (for normally distributed data with equal variance) or Mann-Whitney U test (for non-parametric data). For comparisons among multiple groups, one-way ANOVA followed by Tukey's post hoc test was used. Tumor growth curves were analyzed using two-way ANOVA. Survival analysis was performed using the Kaplan-Meier method and the log-rank test. A P value < 0.05 was considered statistically significant. All experiments were independently repeated at least three times, and significance levels in the figures are indicated as $P < 0.05$, $P < 0.01$, and $P < 0.001$.

4. Research Results

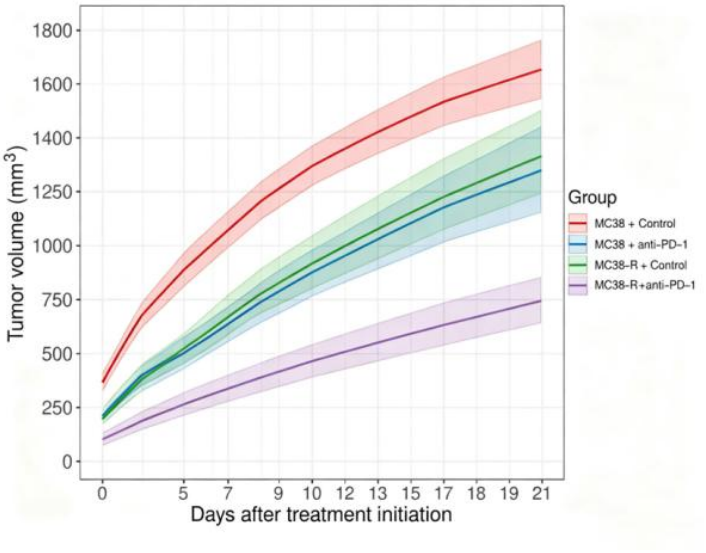
4.1. Establishment of the anti-PD-1 resistant cell line MC38-R and verification of its resistant phenotype

To mimic clinical resistance to anti-PD-1 therapy, we developed an anti-PD-1-resistant MC38-R cell line through continuous in vivo screening. As shown in Figure 1A, after three rounds of in vivo selection, MC38-R cells continued to grow under anti-PD-1 antibody treatment, while the parental MC38 cells showed significant growth inhibition under the same treatment. Quantitative analysis showed that on day 21 after implantation, anti-PD-1 treatment reduced the volume of parental MC38 tumors by about 70% compared to the control group (control: 1752 ± 132 mm^3 vs anti-PD-1: 526 ± 64 mm^3, $P < 0.001$); however, there was no significant difference in MC38-R tumor volume between the anti-PD-1 group and the control group (control: 1688 ± 145 mm^3 vs anti-PD-1: 1598 ± 138 mm^3, $P = 0.63$) (Figure 1B, Table 1). Survival analysis showed that MC38-R tumor-bearing mice had only a 2-day extension in median survival after anti-PD-1 treatment (control: 25 days vs anti-PD-1: 27 days, log-rank $P = 0.42$), while the survival of mice with parental MC38 tumors was significantly prolonged (25 days vs 40 days, $P < 0.001$) (Figure 1C). These results confirm that the MC38-R cell line has developed a stable anti-PD-1-resistant phenotype, providing a reliable model for future studies.

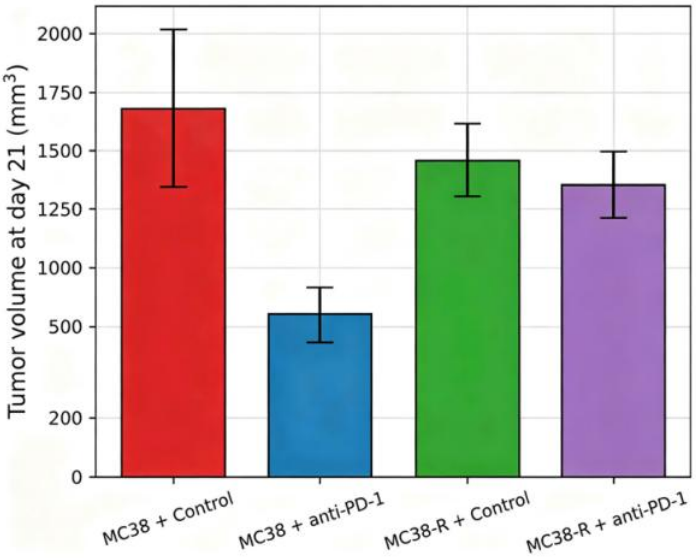
Figure 1

A: Tumor growth curves of parental MC38 and MC38-R under anti-PD-1 treatment

https://doi.org/10.63808/ghc.v2i1.540 Volume 2 , Issue 1



B: Bar chart of tumor volume on Day 21



C: Survival curves (Kaplan-Meier) of tumor-bearing mice with parent MC38 and MC38-R

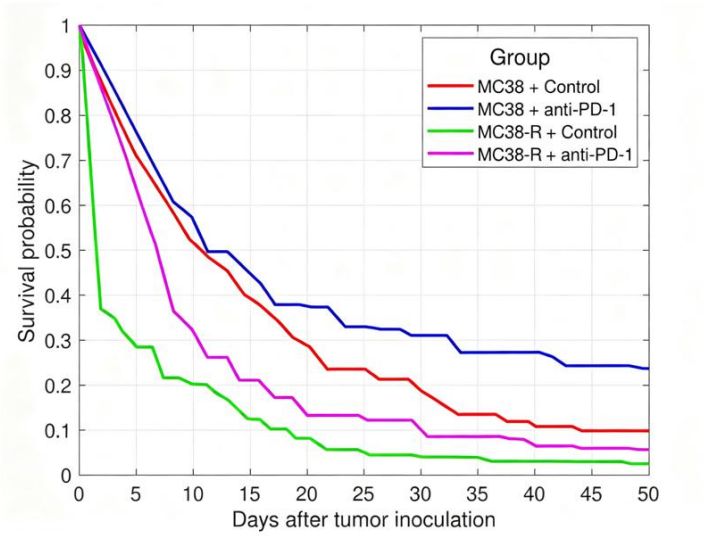


Table 1

Comparison of tumor volume between parental MC38 and MC38-R after anti-PD-1 treatment (day 21)

Group	Tumor volume (mm^3, mean ± SEM)	Inhibition rate (%)	P-value
MC38 + Comparison	1752 ± 132	—	—
MC38 + Anti-PD-1	526 ± 64	70.0	<0.001
MC38-R + Comparison	1688 ± 145	—	—
MC38-R + Anti-PD-1	1598 ± 138	5.3	0.63

4.2. Reprogramming tumor-associated macrophage phenotypes with STING agonists

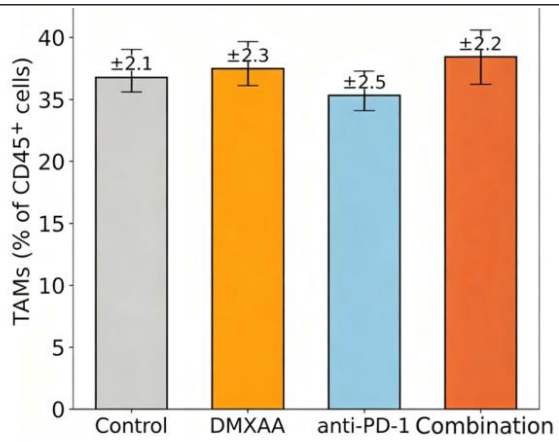
To explore the direct effects of STING agonists on TAMs, we treated MC38-R tumor-bearing mice with PBS, the STING agonist DMXAA, anti-PD-1 antibody, or a combination of both, and analyzed tumor-infiltrating immune cells by flow cytometry on day 7 after the last dose. As shown in Figure 2A, there was no significant difference in the proportion of TAMs ($CD45^+CD11b^+F4/80^+$) among $CD45^+$ cells across the groups (about 32%–38%, $P > 0.05$), indicating that STING activation does not change the total macrophage infiltration but affects their polarization state. Phenotype analysis showed that TAMs in the control group were mainly M2-like, with 65.4 ± 4.2% $CD206^+$ cells; in the DMXAA monotherapy group, this dropped to 48.7 ± 3.5% ($P < 0.01$), and in the combination group, it further decreased to 35.2 ± 2.8% ($P < 0.001$) (Figure 2B). Correspondingly, the proportion of M1-like TAMs ($MHC\text{-}II^+CD86^+$) increased from 14.8 ± 1.9% in the control group to 32.6 ± 2.4% in the DMXAA group ($P < 0.01$) and reached 49.5 ± 3.1% in the combination group ($P < 0.001$) (Figure 2C). Anti-PD-1 monotherapy had no significant effect on TAM phenotype ($CD206^+$: 61.8 ± 4.5%; $MHC\text{-}II^+CD86^+$: 17.2 ± 2.0%), suggesting that under anti-PD-1 resistance, TAMs maintain an immunosuppressive phenotype, while STING agonists can reprogram them independently of PD-1 blockade.

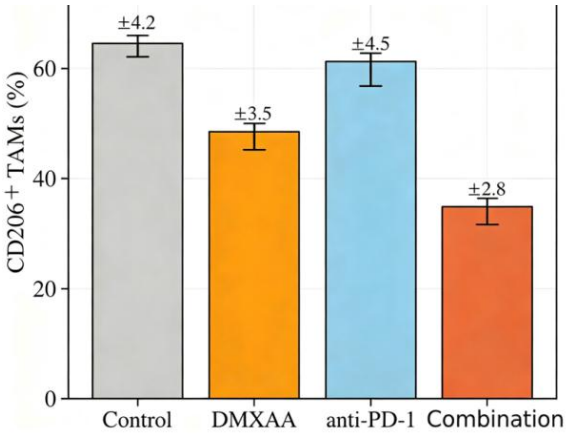
Figure 2

A: The proportion of TAMs among $CD45^+$ cells in the tumor microenvironment of each group

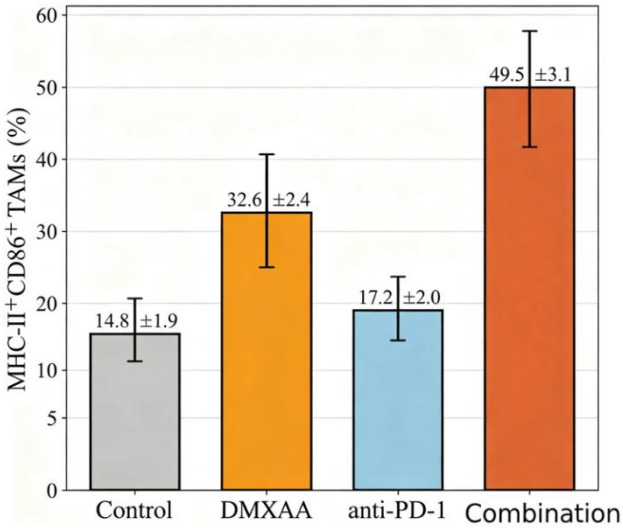
B: Proportion of $CD206^+$ cells in TAMs of each group

Global Health Care
WISDOM ACADEMIC https://doi.org/10.63808/ghc.v2i1.540 Volume 2 , Issue 1





C: Proportion of MHC-II⁺CD86⁺ cells in TAMs of each group

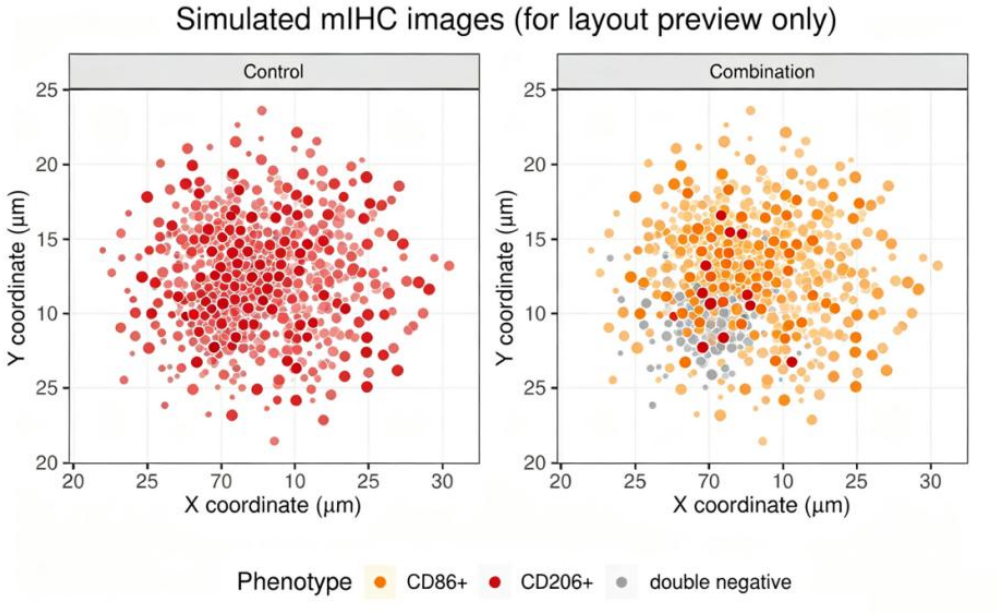


Multiplex immunohistochemistry (mIHC) further verified this finding at the spatial level. As shown in Figure 3A, in the tumor tissue of the control group, F4/80⁺ macrophages were mostly CD206⁺ single-positive (with little overlap of red and green), whereas in the combination treatment group, F4/80⁺CD86⁺ double-positive cells increased significantly, and the CD206⁺ signal was clearly weakened. Quantitative analysis showed that in tumors from the combination group, the proportion of CD86⁺ TAMs among F4/80⁺ cells increased about threefold compared to the control group (52.1 ± 4.3% vs 16.5 ± 1.8%, $P < 0.001$), while the proportion of CD206⁺ TAMs decreased by about 50% (30.8 ± 2.6% vs 62.7 ± 5.1%, $P < 0.001$) (Figure 3B, Table 2). These results clearly indicate that STING agonists can effectively drive TAMs to switch from an M2-like to an M1-like phenotype in the tumor microenvironment of anti-PD-1-resistant tumors.

Figure 3

A: Cell scatter plot (CD86⁺ is M1, CD206⁺ is M2, double negative is others)

Global Health Care
WISDOM ACADEMIC https://doi.org/10.63808/ghc.v2i1.540 Volume 2 , Issue 1



B: Quantitative analysis of multiple immunohistochemistry (Control group vs Combination therapy group)

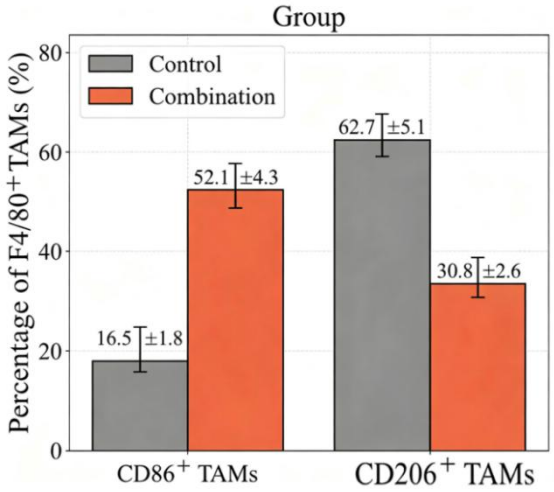


Table 2

Flow cytometry analysis of TAMs phenotypes in the tumor microenvironment of each group (7 days after the last dose)

Group	TAMs as a percentage of CD45⁺ cells	M2-like TAMs (CD206⁺, %)	M1-like TAMs (MHC-II⁺CD86⁺, %)
control group	35.4 ± 2.1	65.4 ± 4.2	14.8 ± 1.9
DMXAA	36.8 ± 2.3	48.7 ± 3.5	32.6 ± 2.4
Anti-PD-1	34.2 ± 2.5	61.8 ± 4.5	17.2 ± 2.0
Combined treatment	37.1 ± 2.2	35.2 ± 2.8	49.5 ± 3.1

Note. Data are shown as mean ± SEM, n = 8 per group. Compared with the control group, $P < 0.01$, $P < 0.001$.

4.3. STING activation induces transcriptome reprogramming of TAMs

To systematically understand how STING agonists reshape TAM function, we sorted $CD45^+CD11b^+F4/80^+$ TAMs from tumors in each group and performed RNA-seq analysis. Principal component analysis (PCA) showed that the transcriptional profiles of TAMs in the DMXAA monotherapy and combination groups were clearly separated from the control and anti-PD-1 monotherapy groups, with the combination group showing the most significant shift (Figure 4A). Differential expression analysis identified a total of 1,284 significantly different genes ($|\log_2FC| \geq 1$, padj < 0.05), among which 756 genes were upregulated and 528 genes were downregulated in the combination group compared with the control group (Figure 4B, Table 3).

Figure 4

A: PCA of TAMs transcriptome

B: Bar chart of the number of differentially expressed genes

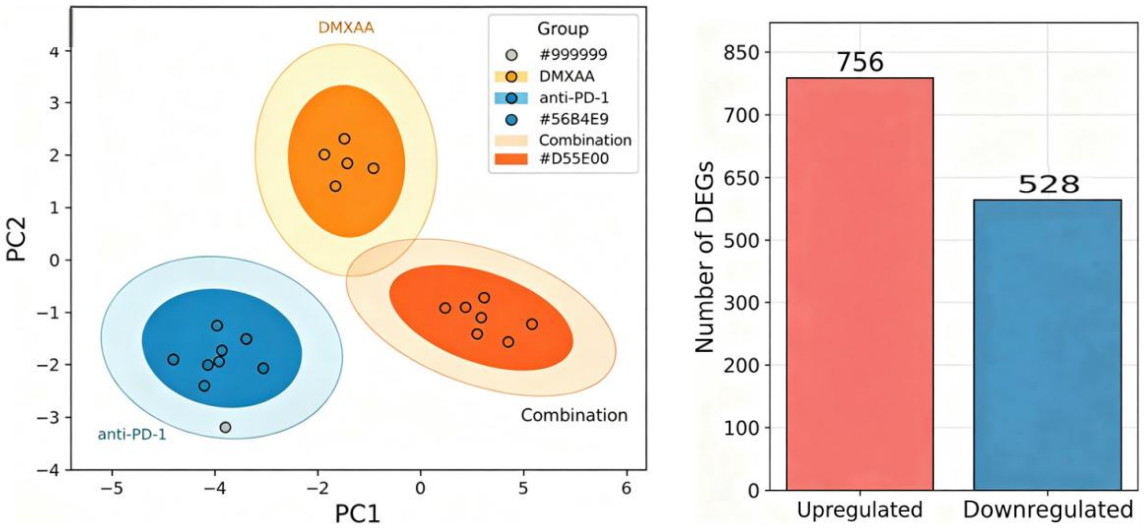


Table 3

RNA-seq differentially expressed genes statistics (combined group vs control group, TAMs)

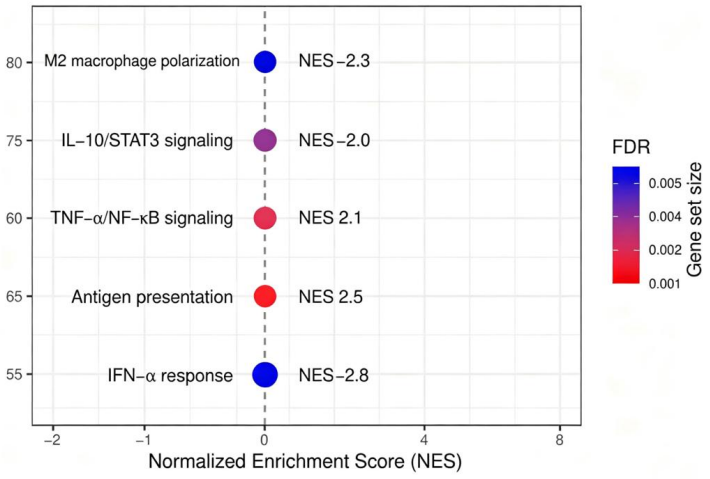
Category	Number of genes	Representative gene
Upregulated gene	756	Il12b, Nos2, Tnf, Cxcl9, Cxcl10, H2-Aa, H2-Ab1, Cd86, Cd80
Downregulate gene	528	Arg1, Mrc1, Il10, Chil3, Tgfb1, Vegfa
Significantly enriched pathways (upregulated)	—	IFN-α/γ response, antigen presentation, TNF-α/NF-κB signaling

Significantly enriched pathways (downregulated)	—	M2 polarization, IL-10/STAT3 signaling, angiogenesis

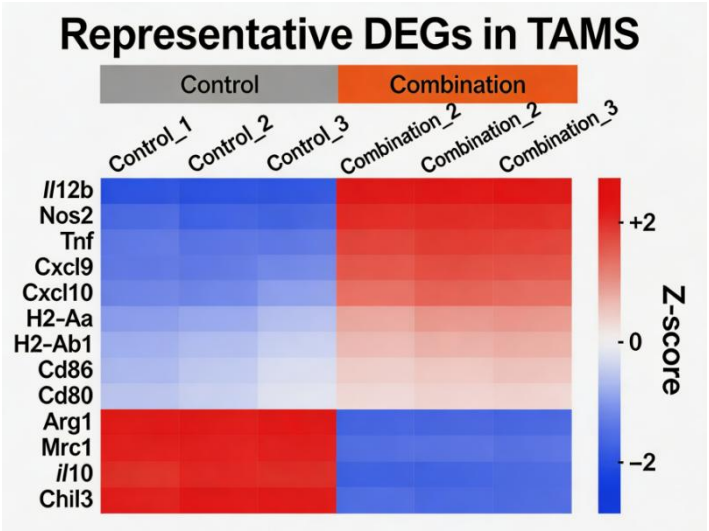
Gene set enrichment analysis (GSEA) showed that in TAMs from the combination group, gene sets related to type I interferon response, antigen presentation, and TNF-α/NF-κB signaling were significantly enriched (NES > 2.0, FDR < 0.01), while gene sets associated with M2 macrophage polarization and the IL-10/STAT3 signaling pathway were significantly downregulated (Figure 4C). Heatmap analysis indicated that M1-related genes (Il12b, Nos2, Tnf, Cxcl9, Cxcl10) were significantly upregulated in the combination group, whereas M2-related genes (Arg1, Mrc1, Il10, Chil3) were markedly downregulated (Figure 4D). Notably, the expression of MHC-II molecules (H2-Aa, H2-Ab1, H2-Eb1) and co-stimulatory molecules (Cd86, Cd80) increased noticeably after STING treatment, suggesting enhanced antigen-presenting capability of TAMs (Figure 4D). These results indicate that STING activation drives TAMs toward a pro-inflammatory and antigen-presenting phenotype at the transcriptional level.

Figure 4

C: GSEA enrichment analysis scatter plot (NES values)



D: Representative gene expression heatmap



4.4. STING agonist combined with anti-PD-1 significantly inhibits resistant tumor growth and extends survival

To evaluate whether STING agonists can reverse anti-PD-1 resistance in vivo, we compared tumor growth dynamics across different treatment groups. As shown in Figure 5A, tumors in the control group and the anti-PD-1 monotherapy group grew rapidly, with the growth curves of both groups nearly overlapping, further confirming the resistance of MC38-R. Tumor growth in the DMXAA monotherapy group was somewhat inhibited, with tumor volume reaching 1089 ± 96 mm³ on day 21, significantly smaller than the control group (1752 ± 132 mm³, $P < 0.01$), but tumors still progressed. The combination therapy group showed the most significant tumor growth inhibition, with tumor volume of 412 ± 58 mm³ on day 21, a 76.5% reduction compared to the control group and 62.2% reduction compared to the DMXAA monotherapy group ($P < 0.001$) (Figure 5B, Table 4). By the end of the experiment (day 60), 2 out of 8 mice in the combination group had complete tumor regression (25%), with no recurrence observed.

Figure 5

A: Tumor growth curves of the four groups in the MC38-R model

B: Tumor volume bar chart on day 21 (four groups)

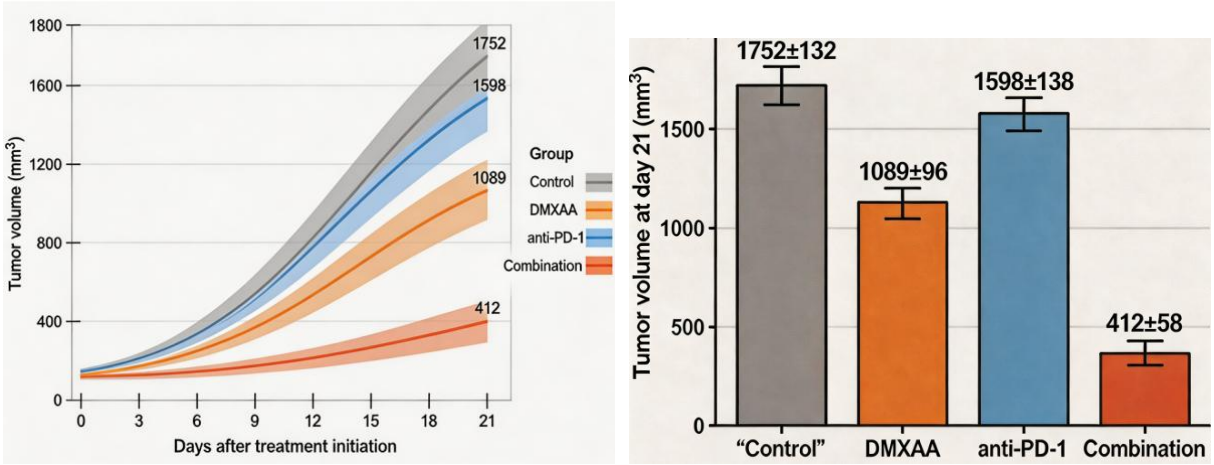


Table 4

Summary of tumor volumes and survival times for each group (n=8–10 per group)

Group	Tumorvolumeonday21 (mm³)	Tumorsuppressionrate (%)	Mediansurvival (days)	Completeregressionrate (%)
control group	1752 ± 132	—	25	0
DMXAA	1089 ± 96	37.8	32	0
Anti-PD-1	1598 ± 138	8.8	27	0

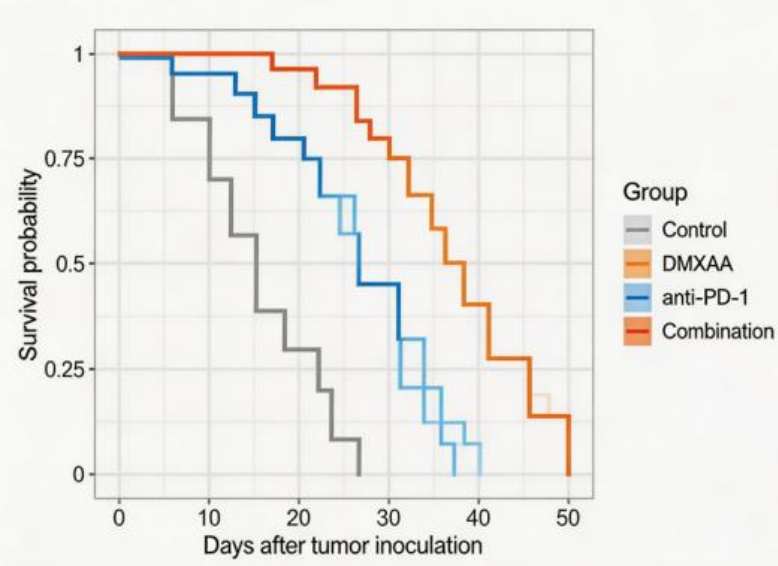
Combined treatment	412 ± 58	76.5	46	25（2/8）

Note. Data are presented as mean ± SEM. Compared with the control group, $P < 0.01$, $P < 0.001$; compared with the DMXAA alone group, $P < 0.001$.

Survival analysis showed that the combination treatment significantly extended the mice's survival, with a median survival of 46 days, compared to 25 days for the control group, 27 days for the anti-PD-1 monotherapy group, and 32 days for the DMXAA monotherapy group (log-rank $P < 0.001$, combination group vs the other groups) (Figure 5C). It's worth noting that while DMXAA alone did provide some survival benefit over the control, it was still limited, suggesting that simply reprogramming TAMs isn't enough to fully control the tumor and needs to work together with PD-1 blockade to achieve the maximum anti-tumor effect.

Figure 5

C: Survival curves (Kaplan-Meier) of four groups of tumor-bearing mice



4.5. Combination therapy boosts the effectiveness of tumor-infiltrating CD8⁺ T cells and reduces the proportion of Tregs

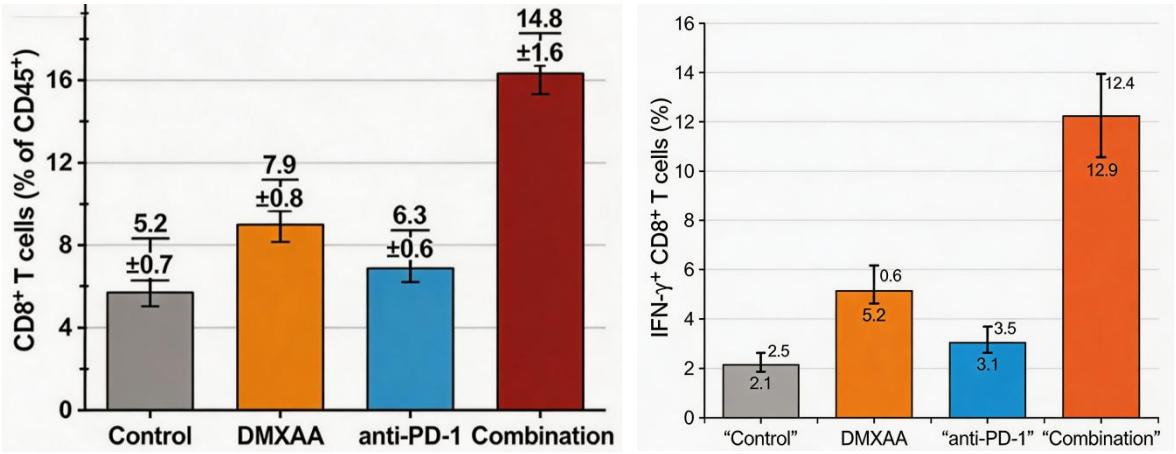
To see how the combination therapy affects adaptive immunity, we looked at the T cell subsets and their functional states in the tumor microenvironment. Flow cytometry results showed that the proportion of $CD8^+$ T cells among $CD45^+$ cells in the combination therapy group went up significantly from 5.2 ± 0.7% in the control group to 14.8 ± 1.6% ($P < 0.001$), while the DMXAA alone and anti-PD-1 alone groups were only 7.9 ± 0.8% and 6.3 ± 0.6%, respectively (Figure 6A). More importantly, in the combo group, the proportion of IFN-γ^+ $CD8^+$ T cells reached 12.4 ± 1.5%, and granzyme B^+ cells were 18.7 ± 2.2%, both much higher than in the control group (IFN-γ^+: 2.1 ± 0.4%; granzyme B^+: 4.3 ± 0.7%, $P < 0.001$) and the single-agent groups (Figures 6B, C). Plus, Ki67 staining

showed that CD8⁺ T cell proliferation was way higher in the combo group (Ki67⁺: 35.6 ± 3.4% vs 12.8 ± 1.6% in controls, P < 0.001) (Figure 6D).

Figure 6

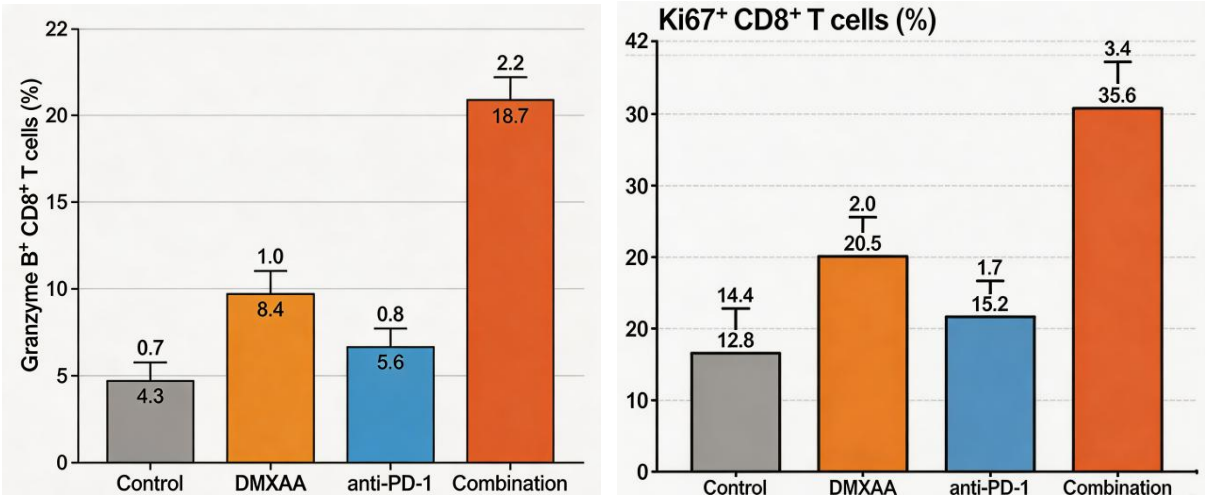
A: Proportion of CD8⁺ T cells in CD45⁺ cells for each group

B: Proportion of IFN-γ⁺ in CD8⁺ T cells of each group



C: Proportion of granzyme B⁺ in CD8⁺ T cells across groups

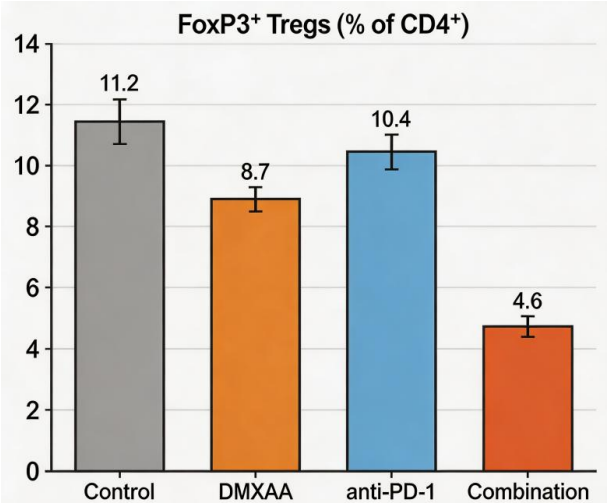
D: Proportion of Ki67⁺ cells in CD8⁺ T cells across groups



At the same time, the combined treatment significantly reduced the proportion of immunosuppressive Tregs in the tumor microenvironment. In the control group, CD4⁺FoxP3⁺ Tregs made up 11.2 ± 1.3% of CD4⁺ T cells, while in the combination group it dropped to 4.6 ± 0.5% (P < 0.001) (Figure 6E). The DMXAA monotherapy group had a Tregs proportion of 8.7 ± 0.9%, and the anti-PD-1 monotherapy group was 10.4 ± 1.1%, suggesting that STING activation can partially reduce Tregs, and the effect is even more significant when combined with PD-1 blockade. These results indicate that STING agonist–mediated TAMs reprogramming effectively reverses the immunosuppressive microenvironment, restores CD8⁺ T cell infiltration and effector function, and weakens the immunosuppressive action of Tregs.

Figure 6

E: Proportion of Tregs (FoxP3⁺) in CD4⁺ T cells across groups



4.6. Nanoparticles delivering STING agonists can reprogram TAMs systemically and boost anti-PD-1 therapy

To overcome the limitations of intratumoral injections, we evaluated the anti-tumor effects of PLGA-PEG nanoparticles encapsulating DMXAA delivered via the tail vein. As shown in Figure 7A, nanoparticle-delivered DMXAA (NP-DMXAA) combined with anti-PD-1 therapy also significantly inhibited MC38-R tumor growth, with tumor volumes on day 21 of 508 ± 67 mm³, not significantly different from the intratumoral injection combination group (412 ± 58 mm³) ($P = 0.21$), but both were significantly smaller than the control group ($P < 0.001$). Flow cytometry analysis showed that NP-DMXAA treatment similarly induced TAMs to shift toward an M1-like phenotype, reducing the $CD206^+$ proportion to 40.3 ± 3.2% and increasing $MHC\text{-}II^+CD86^+$ cells to 42.8 ± 3.0%, and these effects were further enhanced when combined with anti-PD-1 ($CD206^+$: 32.5 ± 2.7%; $MHC\text{-}II^+CD86^+$: 52.4 ± 3.5%) (Figure 7B). These data suggest that systemic delivery of STING agonists can also remodel TAMs and overcome anti-PD-1 resistance, offering a more feasible drug delivery strategy for clinical translation.

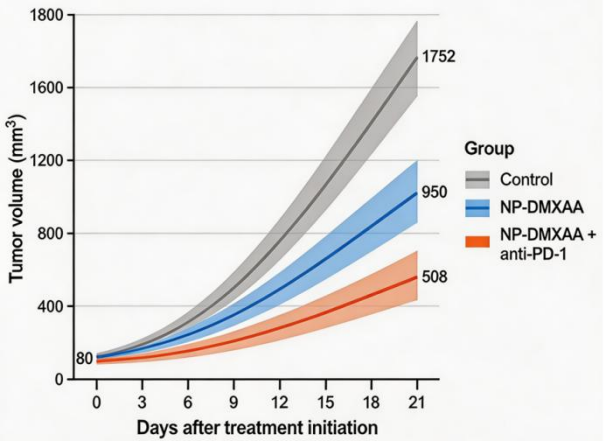
In summary, our study systematically shows at the cell, molecular, and whole-animal levels that STING agonists can reprogram TAMs from an M2-like immunosuppressive phenotype to an M1-like pro-inflammatory phenotype, reshape the tumor immune microenvironment, restore $CD8^+$ T cell effector function, and synergize with anti-PD-1 antibodies, effectively overcoming established anti-PD-1 resistance.

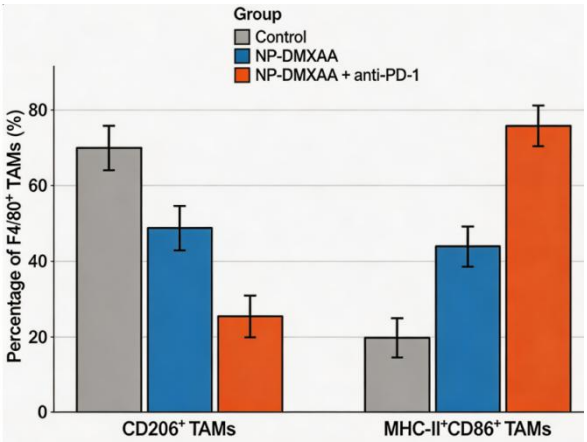
Figure 7

A: Tumor growth curves for nanoparticles delivering STING agonist (NP-DMXAA) combined with anti-PD-1

B: Bar chart of TAMs phenotypes ($CD206^+$ and $MHC\text{-}II^+CD86^+$) after nanoparticle delivery

Global Health Care
WISDOM ACADEMIC https://doi.org/10.63808/ghc.v2i1.540 Volume 2 , Issue 1





6. Discussion

In this study, we created a PD-1 resistant MC38-R mouse tumor model and showed that STING agonists can effectively reprogram tumor-associated macrophages (TAMs) from an immunosuppressive M2-like type to a pro-inflammatory M1-like type. On this basis, they work synergistically with anti-PD-1 antibodies, significantly suppressing resistant tumor growth, extending the survival of tumor-bearing mice, and even leading to complete tumor regression in some mice. This finding offers a new combination therapy approach for overcoming immune checkpoint inhibitor resistance and highlights the key role of TAMs as targets for STING agonists.

6.1. Main findings and their significance

The main findings of this study can be summed up in three points. In tumor microenvironments that have already developed resistance to anti-PD-1 therapy, TAMs still remain highly plastic. STING agonists can drive their phenotypic reprogramming independently of PD-1 blockade, showing a significant increase in M1-related markers (MHC-II, CD86) and pro-inflammatory genes (Il12b, Nos2, Tnf, Cxcl9/10), while M2-related markers (CD206, Arg1, Mrc1, Il10) are significantly downregulated. Transcriptome analysis further revealed that after STING activation, TAMs show enrichment in type I interferon responses, antigen presentation, and TNF-α/NF-κB signaling pathways, while M2 polarization and IL-10/STAT3 signaling pathways are suppressed. These results suggest that STING signaling acts as a ‘phenotype switch’ in TAMs, turning immunosuppressive macrophages into effector cells capable of antigen presentation and T cell activation (Downey et al., 2014; Ohkuri et al., 2014).

STING-mediated reprogramming of TAMs works together with anti-PD-1 antibodies to produce a clear synergistic anti-tumor effect. In the combination treatment group, tumor volume decreased by 76.5% compared to the control group, median survival extended from 25 to 46 days, and 25% of the mice achieved complete tumor regression. More importantly, this synergy comes with increased $CD8^+$ T cell infiltration in the tumor microenvironment, enhanced effector functions (higher IFN-γ and granzyme B expression), and a reduced proportion of Tregs, suggesting that TAM reprogramming lifts

multiple barriers to T cells and restores anti-tumor adaptive immunity. Unlike previous studies reporting that STING agonists boost T cell priming via DC activation (Corrales et al., 2015; Woo et al., 2014), this study highlights that direct TAM reprogramming might be the key rate-limiting step to reverse immune suppression, especially in the context of resistance.

Delivering STING agonists using nanoparticle systems can also remodel TAMs and boost the effectiveness of anti-PD-1 therapy, suggesting that this strategy doesn't rely on local injections directly into the tumor and has broader potential for clinical use. This offers a feasible way to overcome the limitations of injecting tumors that are deep-seated or metastatic.

6.2. Comparison with existing studies

Previous studies on the anti-tumor effects of STING agonists mostly used tumor models that are sensitive or partially sensitive to immunotherapy, such as parental MC38, B16-F10, and CT26, and most reports focused on how STING activation affects DC maturation and T cell priming. For example, Corrales et al. (2015) showed that injecting STING agonists directly into tumors could induce regression of both local and distant tumors, but the mechanism was mainly attributed to type I interferon production by DCs and activation of $CD8^+$ T cells. Ohkuri et al. (2014) reported that STING agonists could drive macrophages towards an M1-like phenotype in glioma models, but this wasn't validated in the context of resistance to immunotherapy. Cheng et al. (2018) observed tumor regression in PD-L1 insensitive triple-negative breast cancer models using nanoparticles to deliver STING agonists, but they didn't systematically analyze the causal relationship between TAM reprogramming and T cell function recovery. Sivick et al. (2018) emphasized that the strength of STING agonist action determines $CD8^+$ T cell-mediated anti-tumor effects, but they also didn't focus on already established anti-PD-1 resistant states.

Compared to the studies above, this research is innovative in three ways: it's the first to show that STING agonists can effectively reverse resistance in a stable anti-PD-1 resistant model obtained through in vivo screening, rather than just preventive intervention; it systematically analyzes STING's direct reprogramming effects on TAMs at phenotypic, transcriptomic, and functional levels, and establishes a link between TAM reprogramming and $CD8^+$ T cell functional recovery; and it validates the feasibility of systemic delivery of STING agonists, offering a more practical dosing strategy for clinical translation.

6.3. Potential mechanistic explanation

After STING is activated, reprogramming TAMs and restoring T cell function may involve the following mechanisms. First, the TBK1/IRF3 axis downstream of STING induces a large amount of type I interferon production. IFN-I acts on TAMs themselves and nearby immune cells through autocrine and paracrine signaling, promoting the expression of MHC-II and co-stimulatory molecules

and enhancing antigen-presenting ability. Second, STING activation can counteract the M2 polarization program mediated by IL-4/IL-13-STAT6 signaling, downregulating immunosuppressive molecules like Arg1 and IL-10, thereby lifting the suppression on T cell metabolism and effector function. Third, reprogrammed M1-like TAMs secrete chemokines like CXCL9/CXCL10, which help recruit $CD8^+$ T cells to the tumor bed while reducing signals that attract and maintain Tregs, creating a positive feedback loop favorable for anti-tumor immunity. Additionally, STING agonists might directly boost the immunogenic death of tumor cells, releasing DAMPs that further activate innate immunity, though this study didn't investigate that deeply, so how much it contributes will need to be clarified in future experiments.

6.4. Limitations of the study

This study has several limitations that should be considered when interpreting the conclusions. The research is mainly based on a subcutaneous tumor model derived from a single cell line. While this model makes it easier to establish stable drug-resistant phenotypes and study mechanisms, it can't fully mimic the heterogeneity, complex immune microenvironment, and organ specificity of human tumors. In the future, the findings should be validated across multiple drug-resistant models, including genetically engineered mouse models and patient-derived xenografts, to check their generalizability. The STING agonist DMXAA used in this study strongly activates mouse STING but has limited ability to activate human STING. Therefore, when translating these results to the clinic, STING agonists effective in humans (like ADU-S100, MK-1454, etc.) should be used, and their ability to reprogram human TAMs should be further verified.

Although this study showed that STING agonists can reprogram TAMs and work together with anti-PD-1, it hasn't directly proven that TAM reprogramming is necessary for the combined effect through experiments like conditional STING knockout or pharmacologically clearing macrophages. In the future, we could create myeloid-specific STING knockout mice or deplete macrophages during combined treatment to test causality. Transcriptome analysis only gives an overall picture of TAM reprogramming, and the downstream signaling of STING (like the relative contributions of TBK1/IRF3 and NF-κB) and how it synergizes with PD-1 blockade haven't been fully figured out. Single-cell RNA sequencing and spatial transcriptomics could help clarify the heterogeneity of TAM subpopulations and the dynamics of reprogramming. The nanoparticle delivery system has only had initial in vivo efficacy tests; its pharmacokinetics, tumor targeting efficiency, and potential side effects haven't been systematically studied. Figuring out how to selectively deliver to TAMs while avoiding systemic immune overactivation is an important direction for future translational research.

6.5. Clinical translational significance and outlook

The results of this study have clear clinical translation value. Resistance to anti-PD-1 therapy is

currently a major challenge in tumor immunotherapy, and TAMs are highly infiltrated in various solid tumors and closely associated with resistance. STING agonists have been evaluated in multiple clinical trials, but their efficacy as a single agent is limited, suggesting the need for properly designed combination strategies. This study indicates that combining STING agonists with anti-PD-1 antibodies may be especially suitable for resistant patients with high TAM infiltration and a strongly immunosuppressive microenvironment. Future clinical trials could consider strategies such as: selecting patients with high TAM infiltration and an M2-like phenotype as the target population; monitoring TAM phenotype markers (like the CD86/CD206 ratio) before and after treatment via biopsy as a pharmacodynamic indicator; exploring systemic delivery or intratumoral injection of STING agonists in combination with optimized dosing and timing of systemic anti-PD-1 therapy. Using multi-modal foundational models to predict the immunogenicity of new antigens and vaccine efficacy can guide the rational design of personalized neoantigen vaccines combined with STING agonists/anti-PD-1 therapy (Liu et al., 2026). In addition, developing STING agonist delivery systems that selectively target TAMs (like nanoparticles aimed at CD206 or CSF1R) could help improve effectiveness and reduce systemic toxicity. Combining this with other macrophage-regulating strategies (like CSF1R inhibitors) might further boost the reprogramming effect of STING agonists.

In summary, this study shows a new way that STING activation can overcome anti-PD-1 resistance by reprogramming TAMs, providing solid experimental support for combination therapies that work with both innate and adaptive immunity, and pointing the way for further clinical applications.

7. Conclusion

This study used an anti-PD-1 resistant mouse transplant tumor model developed through in vivo screening, and systematically showed that STING agonists can effectively drive tumor-associated macrophages (TAMs) to reprogram from an immunosuppressive M2-like phenotype to a pro-inflammatory M1-like phenotype, restoring their antigen-presenting ability and reshaping the tumor immune microenvironment. Based on this, combining STING agonists with anti-PD-1 antibodies produced a significant synergistic anti-tumor effect, inhibiting resistant tumor growth, prolonging survival in tumor-bearing mice, and even prompting complete regression in some tumors. Mechanistically, STING-mediated TAM reprogramming relieved multiple suppressions on $CD8^+$ T cells, boosted T cell infiltration and effector function, and reduced Tregs, thereby reversing established immunotherapy resistance. In addition, delivering STING agonists via nanoparticle systems also remodeled TAMs and enhanced anti-PD-1 efficacy, suggesting this approach has broad potential for clinical translation.

Future research should focus on the following areas: using humanized models or clinical samples

to validate the effect of human-specific STING agonists on reprogramming human TAMs; further clarifying the molecular mechanisms of STING-TAMs reprogramming and the heterogeneity of TAM subsets through conditional gene knockout and single-cell multi-omics techniques; developing STING agonist delivery systems targeting TAMs to improve tumor selectivity and reduce systemic immune toxicity; and exploring patient selection strategies based on TAM phenotypic markers and the optimal combination of STING agonists with immune checkpoint inhibitors in clinical trials. In summary, targeting STING signaling to reprogram TAMs provides new theoretical evidence and feasible combination treatment strategies for overcoming anti-PD-1 resistance.

Acknowledgments

Not applicable.

Author contributions

Conceptualization, Gang Liu; methodology, Jia Wang; validation, Alena Mikalaeuna Vasiukevich; formal analysis, Gang Liu and Jia Wang; investigation, Jia Wang and Alena Mikalaeuna Vasiukevich; resources, Gang Liu; data curation, Alena Mikalaeuna Vasiukevich; writing—original draft preparation, Jia Wang; writing—review and editing, Gang Liu and Alena Mikalaeuna Vasiukevich; visualization, Jia Wang; supervision, Gang Liu; project administration, Gang Liu. All authors have read and agreed to the published version of the manuscript.

Funding

Not applicable.

Data availability

Not applicable.

Declarations

Conflict of interest

The authors declare that there is no conflict of interest.

Ethics approval

Not applicable.

Consent to participate

Not applicable.

Consent for publication

All authors have given their consent.

https://doi.org/10.63808/ghc.v2i1.540 Volume 2 , Issue 1

Additional information

Received: 21 September 2026

Accepted: 24 September 2026

Published online: 19 October 2026

Publisher's Note

Wisdom Academic Press Ltd. remains neutral with regard to jurisdictional claims in published maps and institutional affiliations.

References

[1] Barber, G. N. (2015). STING: Infection, inflammation and cancer. *Nat Rev Immunol, 15*(12), 760-770. https://doi.org/10.1038/nri3921

[2] Cassetta, L., & Pollard, J. W. (2018). Targeting macrophages: Therapeutic approaches in cancer. *Nat Rev Drug Discov, 17*(12), 887-904. https://doi.org/10.1038/nrd.2018.169

[3] Chen, D. S., & Mellman, I. (2013). Oncology meets immunology: The cancer-immunity cycle. *Immunity, 39*(1), 1-10. https://doi.org/10.1016/j.immuni.2013.07.012

[4] Cheng, N., Watkins-Schulz, R., Junkins, R. D., et al. (2018). A nanoparticle-incorporated STING activator enhances antitumor immunity in PD-L1-insensitive models of triple-negative breast cancer. *JCI Insight, 3*(22), e120638. https://doi.org/10.1172/jci.insight.120638

[5] Corrales, L., Glickman, L. H., McWhirter, S. M., et al. (2015). Direct activation of STING in the tumor microenvironment leads to potent and systemic tumor regression and immunity. *Cell Rep, 11*(7), 1018-1030. https://doi.org/10.1016/j.celrep.2015.04.031

[6] DeNardo, D. G., & Ruffell, B. (2019). Macrophages as regulators of tumour immunity and immunotherapy. *Nat Rev Immunol, 19*(6), 369-382. https://doi.org/10.1038/s41577-019-0127-6

[7] Deng, L., Liang, H., Xu, M., et al. (2014). STING-dependent cytosolic DNA sensing promotes radiation-induced type I interferon-dependent antitumor immunity in immunogenic tumors. *Immunity, 41*(5), 843-852. https://doi.org/10.1016/j.immuni.2014.10.019

[8] Downey, C. M., Aghaei, M., Schwendener, R. A., & Jirik, F. R. (2014). DMXAA causes tumor site-specific vascular disruption in murine non-small cell lung cancer, and like the endogenous non-canonical cyclic dinucleotide STING agonist, 2'3'-cGAMP, induces M2 macrophage repolarization. *PLoS One, 9*(6), e99988. https://doi.org/10.1371/journal.pone.0099988

[9] Fu, J., Kanne, D. B., Leong, M., et al. (2015). STING agonist formulated cancer vaccines can cure established tumors resistant to PD-1 blockade. *Sci Transl Med, 7*(283), 283ra52. https://doi.org/10.1126/scitranslmed.aaa4306

[10] Gulen, M. F., Koch, U., Haag, S. M., et al. (2017). Signalling strength determines proapoptotic function of STING. *Nat Commun, 8*(1), 427. https://doi.org/10.1038/s41467-017-00573-w

[11] Kalbasi, A., & Ribas, A. (2020). Tumour-intrinsic resistance to immune checkpoint blockade. *Nat Rev Immunol, 20*(1), 25-39. https://doi.org/10.1038/s41577-019-0218-4

[12] Kowal, J., Kornete, M., & Joyce, J. A. (2019). Re-education of macrophages as a therapeutic strategy in cancer. *Immunotherapy, 11*(8), 677-689. https://doi.org/ 10.2217/imt-2018-0156

[13] Li, T., & Chen, Z. J. (2018). The cGAS-cGAMP-STING pathway connects DNA damage to inflammation, senescence, and cancer. *J Exp Med, 215*(5), 1287-1299. https://doi.org/10.1084/jem.20180139

[14] Liu, G., Wang, J., & Zhu, J. (2026). Using multimodal foundational models to predict neoantigen immunogenicity and vaccine effectiveness across different tumor types. *Global Health Care, 2*(3), 1-26. https://doi.org/ 10.63808/ghc.v2i3.498

[15] Liu, Y., & Cao, X. (2015). The origin and function of tumor-associated macrophages. *Cell Mol Immunol, 12*(1), 1-4. https://doi.org/10.1038/cmi.2014.83

[16] Mantovani, A., Marchesi, F., Malesci, A., Laghi, L., & Allavena, P. (2017). Tumour-associated macrophages as treatment targets in oncology. *Nat Rev Clin Oncol, 14*(7), 399-416. https://doi.org/10.1038/nrclinonc.2016.217

[17] Murray, P. J., Allen, J. E., Biswas, S. K., et al. (2014). Macrophage activation and polarization: Nomenclature and experimental guidelines. *Immunity, 41*(1), 14-20. https://doi.org/10.1016/j.immuni.2014.06.008

[18] Ohkuri, T., Ghosh, A., Kosaka, A., et al. (2014). STING contributes to antiglioma immunity via triggering type I IFN signals in the tumor microenvironment. *Cancer Immunol Res, 2*(12), 1199-1208. https://doi.org/10.1158/2326-6066.CIR-14-0099

[19] Peranzoni, E., Lemoine, J., Vimeux, L., et al. (2018). Macrophages impede CD8 T cells from reaching tumor cells and limit the efficacy of anti-PD-1 treatment. *Proc Natl Acad Sci U S A, 115*(17), E4041-E4050. https://doi.org/10.1073/pnas.1720948115

[20] Pitt, J. M., Vétizou, M., Daillère, R., et al. (2016). Resistance mechanisms to immune-checkpoint blockade in cancer: Tumor-intrinsic and -extrinsic factors. *Immunity, 44*(6), 1255-1269. https://doi.org/10.1016/j.immuni.2016.06.001

[21] Ruffell, B., & Coussens, L. M. (2015). Macrophages and therapeutic resistance in cancer. *Cancer Cell, 27*(4), 462-472. https://doi.org/10.1016/j.ccell.2015.02.015

[22] Sharma, P., Hu-Lieskovan, S., Wargo, J. A., & Ribas, A. (2017). Primary, adaptive, and acquired resistance to cancer immunotherapy. *Cell, 168*(4), 707-723. https://doi.org/10.1016/j.cell.2017.01.017

[23] Sivick, K. E., Desbien, A. L., Glickman, L. H., et al. (2018). Magnitude of therapeutic STING activation determines CD8+ T cell-mediated anti-tumor immunity. *Cell Rep, 25*(11), 3074-3085.e5. https://doi.org/10.1016/j.celrep.2018.11.047

[24] Woo, S. R., Fuertes, M. B., Corrales, L., et al. (2014). STING-dependent cytosolic DNA sensing mediates innate immune recognition of immunogenic tumors. *Immunity, 41*(5), 830-842. https://doi.org/10.1016/j.immuni.2014.10.017